Journal of Physics and Chemistry of Solids 69 (2008) 3052–3057

Contents lists available at ScienceDirect

Journal of Physics and Chemistry of Solids

journal homepage: www.elsevier.com/locate/jpcs

Charge dynamics and optical properties of layered cobaltates

J. Dong [a], D. Wu [a], J.L. Luo [a], M.E. Li [a,b], X.G. Luo [b], X.H. Chen [b], R. Jin [c], D. Mandrus [c], N.L. Wang [a,*]

[a] Beijing National Laboratory for Condensed Matter Physics, Institute of Physics, Chinese Academy of Sciences, P.O. Box 603, Beijing 100080, China
[b] Hefei National Laboratory for Physical Science at Microscale, University of Science and Technology of China, Hefei 230026, China
[c] Materials Science and Technology Division, Oak Ridge National Laboratory, Oak Ridge, TN 37831, USA

ARTICLE INFO

PACS:
78.20.−e
71.27.+a
74.25.Gz
74.25.Kc

Keywords:
A. Electronic materials
C. Infrared spectroscopy
D. Optical property

ABSTRACT

We study the charge dynamics and electronic structure by optical spectroscopy technique. Here we focus on the following four issues: (1) the evolution of optical spectra with Na content; (2) the spectral features specific to different regions in the phase diagram; (3) the *c*-axis optical response for crystal at the A-type antiferromagnetic region; (4) the optical response of misfit-layered $Bi_2M_2Co_2O_y$ (M = Ba, Sr, Ca) and $Ca_3Co_4O_y$ single crystals.

1. Introduction

Layered Na_xCoO_2 system has generated great interests in the condensed matter community for it realizes a triangular lattice with partially filled strongly correlated electronic states. Na donates its electron to the CoO_2 layer, hence Na content controls the doping level. A rich phase diagram has been revealed for Na_xCoO_2 with a change of Na content x. A spin ordered phase is found for $x>0.75$. With decreasing Na contents, the material becomes a "Curie–Weiss metal" for x near 0.7, then a charge-ordered insulator with $x\sim0.5$, and finally a paramagnetic metal with $x\sim0.3$ [1]. Superconductivity occurs when sufficient water is intercalated between the CoO_2 layers for x near 0.3. The layered cobaltate provides a model system for studying the physics of correlated electrons in a 2D triangular lattice. It is also widely expected that the study of Na_xCoO_2 system may shed new light on high-T_c superconductivity in cuprates.

Soon after the discovery of superconductivity in hydrated Na_xCoO_2 [2], many researchers tend to consider the system as a doped Mott insulator just like the case of cuprate superconductors. The picture was formed based on the assumption that the $x=0$ end member is a Mott insulator, and Na intercalations introduce electrons to the system. In CoO_2, the valence state of Co is 4+, there are five electrons in 3d orbitals. Under octahedral crystal field, the 3d manifold is split into t_{2g} and e_g orbitals. The trigonal configuration will further split the t_{2g} orbitals into a_{1g} and a doublet e'_g [3]. With five electrons in such split t_{2g} shell, the $x=0$ compound could be a Mott insulator if the electron correlation is strong enough. Experimentally, the above assumption was never justified [4]. On the other hand, the $x=1$ end member has six electrons in the 3d orbitals and would be a band insulator due to the fully filled t_{2g} bands and completely empty e_g bands. Then, the metallic Na_xCoO_2 with $0<x<1$ can also be viewed as a doped band insulator with a hole concentration of $(1-x)$. Judging whether the system is a doped Mott insulator or a doped band insulator is a very important issue, as it is a starting point to understand the system with complex phase diagram.

Besides Na_xCoO_2, there is a series of cobalt oxides, Bi–M–Co–O (M = Ba, Sr, Ca), which contain CoO_2 layers in the structure. In early work, those oxides were considered to have the same structure as the cuprate superconductor $Bi_2Sr_2CaCu_2O_{8+\delta}$ [5,6]. It was realized by subsequent studies that those oxides have misfit-layered structure [7], i.e. it consists of alternate stacking of four rock-salt BiMO layers and one hexagonal CoO_2 layer [7–9]. Another well-known misfit-layered cobaltate is $Ca_3Co_4O_9$, where a hexagonal CoO_2 layer is intercalated between triple rock-salt Ca_2CoO_3 layers [10]. As those compounds share common hexagonal CoO_2 layer in the structures, it would be very interesting to compare their physical properties with those of Na_xCoO_2 system.

Optical spectroscopy is a powerful technique to probe the charge excitation and dynamics. Unlike angular resolved photoemission spectroscopy (ARPES) which is sensitive to surface, optical measurement probes bulk property. A number of optical spectroscopy studies have been done on this system [11–17]. In this proceedings paper, we would first summarize our measurement

* Corresponding author. Tel.: +86 10 8264 9584.
E-mail address: nlwang@aphy.iphy.ac.cn (N.L. Wang).

0022-3697/$ - see front matter © 2008 Elsevier Ltd. All rights reserved.
doi:10.1016/j.jpcs.2008.06.115

results on the doping evolution [16,17]. This provides a way to resolve the important issue whether the system should be considered as a doped Mott insulator or a doped band insulator. Then, we address several notable spectral features at different doping regimes in the phase diagram. We shall also present new data on the *c*-axis response of $x = 0.85$ crystal, as well as on the misfit-layered compounds $Bi_2M_2Co_2O_y$ (M = Ba, Sr, Ca) and $Ca_3Co_4O_y$.

2. The evolution of optical spectra with Na content

The single crystal samples of Na_xCoO_2 were grown by floating zone method. For as-grown crystals, the Na content could be in the range of $x = 0.70$–0.92. Deintercalation of Na was achieved by immersing the as-grown crystals in solution of different ratios of bromine/CH_3CN. Then, a series of crystals with reduced Na concentrations $x = 0.48$, 0.36, 0.32, 0.18 determined by ICP measurement were obtained [17]. Fig. 1(a) and (b) show the room temperature in-plane reflectance and conductivity spectra for Na_xCoO_2 with $x = 0.18-0.92$ over broad frequencies [17]. We found that the compound with the highest Na content has the lowest reflectance values and edge frequency, as a result, it has the lowest spectral weight in optical conductivity curve. According to the partial sum-rule, the area under the conductivity curve below a certain frequency corresponds to the effective carrier density below that frequency. The effective density of carriers per Co ion contributed to conductivity below ω is $(m/m_b)N_{eff}(\omega) = (2mV_{cell}/\pi e^2 N)\int_0^{\omega}\sigma(\omega')\,d\omega'$, where m is the free-electron mass, m_b the averaged high-frequency optical or band mass, V_{cell} a unit cell volume, N the number of Co ions per unit volume. Fig. 1(c) displays $(m/m_b)N_{eff}$ as a function of frequency for those samples. Obviously, the compound with high Na content has low conducting carrier density. The gradually vanishing spectral weight for high Na content samples confirms the band insulator for $x = 1$ compound. With reducing the sodium content from 0.92 to 0.18, the spectral weight increases monotonously, suggesting a continuous increase of the effective carriers density. The optical data indicate that at least down to $x = 0.18$, the effective carrier density still increases with decreasing Na content. The doping evolution strongly suggests a doped band insulator picture rather than a doped Mott insulator [16,17]. Consistent with our data, recent NMR study on CoO_2 compound revealed a metallic state with a moderately electron correlation [18]. As the magnetic phase mainly appears in the region with higher Na contents, the electron correlation is even stronger in those region than in the low Na region. This has motivated several theoretical studies on this Na-induced correlations [19,20].

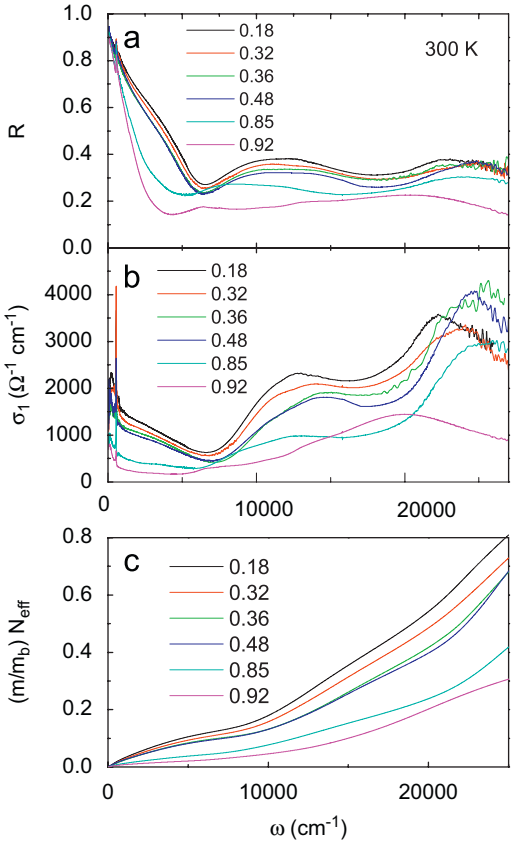

Fig. 1. (a) and (b) show the doping evolution of in-plane reflectance and conductivity of Na_xCoO_2 at room temperature over broad frequencies. Panel (c) displays the effective carrier density of Co ion for different sodium contents [17].

It would be interesting to compare the spectral evolution as revealed by optics with that of ARPES. According to band structure calculations [3,21,22], both the a_{1g} and the e'_g bands should cross the Fermi level, producing a large Fermi surface (FS) around Γ point and small hole pockets near K points in the Brillouin zone, respectively. However, the ARPES experiments [23–26] indicated that only the a_{1g} FS exists, while the e'_g bands sink below the Fermi level for different compositions. As indicated above, optical spectroscopy revealed unambiguously a monotonous decrease of the effective carrier number with increasing Na contents, whereas the ARPES indicated a non-monotonous change of the area enclosed by the a_{1g} FS with Na content. The FS was reported to decrease with increasing Na content from 0.3 to 0.7. However, the FS becomes large when the system goes into the magnetic ordering region ($x \geqslant 0.75$) [25]. As the magnetic moments are ferromagnetic correlated within the plane, it is likely that the exchange splitting of the spin-up and spin-down bands occurs and there is only one spin polarized band crossing E_F. Spin polarized ARPES is required to resolve this important issue.

3. Specific features in different Na doping regions

In the phase diagram, the two metallic regions are separated by a charge ordering insulating phase near $x = 0.5$. We shall first look at the spectral features in those two regions. Fig. 2 shows the *T*-dependent in-plane optical conductivity at low frequency for two different compositions: (a) $x = 0.18$ and (b) $x = 0.85$. $x = 0.18$ is the lowest Na content achieved. The $x = 0.85$ sample is metallic down to 20 K, below which its *T*-dependent dc resistivity shows an upturn due to the so-called A-type magnetic ordering. Other compounds with Na contents below 0.5 are more or less similar to $x = 0.18$ sample, while those with Na contents above 0.5 are similar to $x = 0.85$ sample. For $x = 0.18$ sample, the most striking feature is that the $\sigma_1(\omega)$ is gradually suppressed roughly below 2000 cm^{-1} with decreasing T from 300 K. Such suppression was usually taken as a signature of a pseudogap in $\sigma_1(\omega)$ spectra. The spectral structure resembles significantly the hope-doped cuprates in the pseudogap state. Although it is known that the coupling of electrons with a bosonic mode could lead to similar spectral structure, our analysis indicated that the suppression in the density of states is essential in the present cobaltate compound [17]. It is very difficult to understand such spectral feature, since there is no signature of any gap on the FS centered at Γ point. It is likely that the *PG*-like phenomenon is purely a band structure effect, i.e. the interband transition from occupied e'_g band to empty part of a_{1g} band within t_{2g} manifold [12,27].

For $x = 0.85$ sample, similar suppression is also present in $\sigma_1(\omega)$, but appears at higher energy, about 3000–4000 cm^{-1}.

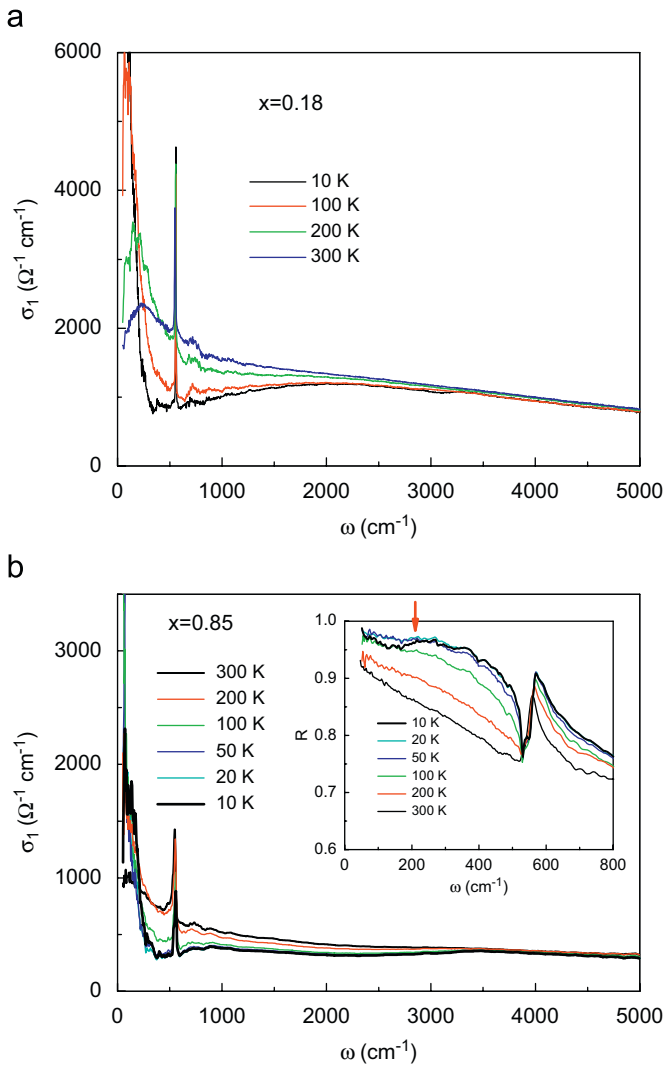

Fig. 2. In-plane optical conductivity of Na_xCoO_2 with $x = 0.18$ (a) and $x = 0.85$ (b) at different temperatures. Inset of (b) shows the T-dependent reflectance spectra. The red arrow indicates the energy scale below which the low-T ($T < 20$ K) reflectance is suppressed.

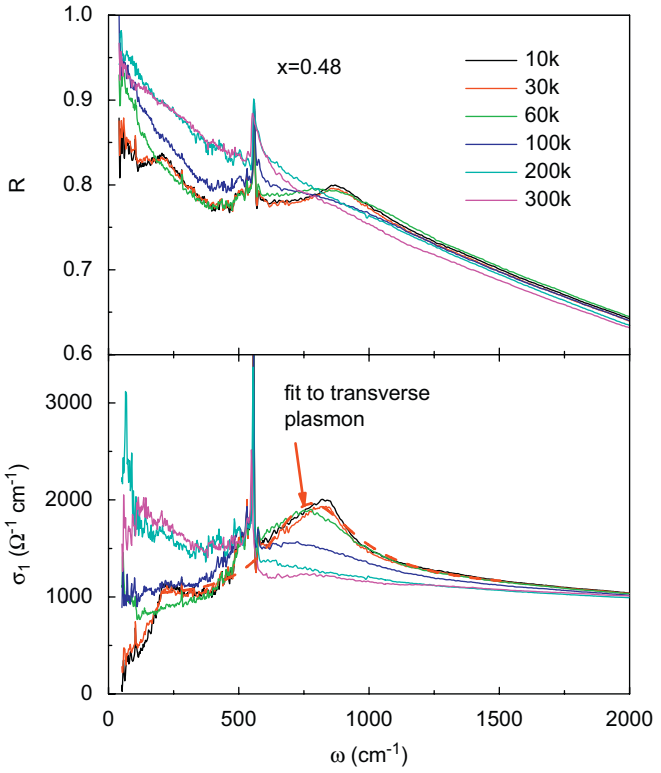

Fig. 3. T-dependent R and $\sigma_1(\omega)$ spectra for $x = 0.48$ crystal at different temperatures. The red dash curve is the fitting curve of the low-T optical conductivity to the transverse plasmon model, Eq. (1).

Indeed, if we compare with band structure calculation and ARPES measurement results [26], the e'_g band sinks further below the Fermi level, resulting in an increase of the interband transition energy within t_{2g} manifold. For $x = 0.85$ sample, there exists another prominent feature, that is, when the compound enters into the magnetic ordering phase (below ~20 K), the low-frequency optical conductivity is suppressed. In fact, the suppression can be more clearly seen in reflectance spectrum below 230 cm^{-1} as shown in the inset of Fig. 2(b). This is consistent with the dc resistivity measurement which shows an upturn below 20 K.

For the charge ordering sample with Na content x~0.5 composition, Na orders in an orthorhombic superlattice commensurate with the Co lattice. As the valence state of Co depends on the Co positions relative to Na ions, the Na orderings would induce charge orderings in Co layers, which was observed at low T as a sharp metal–insulator transition occurs at $T_{MIT} = 50$ K [1]. In addition, a long range magnetic ordering appears at higher temperature $T_N = 87$ K. Neutron scattering experiments revealed that the $Co^{3.5+\delta}/Co^{3.5-\delta}$ ions order into stripes within the CoO_2 planes with alternating rows of ordered and non-ordered Co ions below T_N [28,29].

Fig. 3 shows the T-dependent reflectance and conductivity spectra for x close to 0.5 (the ICP measurement indicates $x = 0.48$) crystal. The conductivity spectra show two prominent features at low temperature. One is the gap formation at low T. The almost complete suppression of the spectral weight at low T suggests a full gap in the FS. The temperature-dependent measurement indicated that the gap opens just below T_{MIT}, so the gap is linked with the charge-ordering, not related to the magnetic ordering appearing at higher T. It is noted that the gap is small, only ~15 meV (125 cm^{-1}) in optics [16]. Another one is the emergence of a peak/resonance mode structure in conductivity near 800 cm^{-1}. A weak feature, or a hump, is already evident at 100 K, a temperature much higher than magnetic ordering or charge ordering transition temperature, and gains further spectral weight at lower T. The origin of this mode is not clear. In our earlier work, we correlated the feature with the possible formation of polarons due to strong electron–phonon coupling [16]. A more likely explanation for this phenomenon is that it is a transverse plasma resonance associated with a coupling between two different charge stripes formed by $Co^{3.5+\delta}$ and $Co^{3.5-\delta}$, respectively. The transverse plasmon, which gives a peak at finite frequency in optical conductivity, was observed and thoroughly studied in the c-axis ($\boldsymbol{E}\|c$-axis) optical response of multilayered cuprates [30–33]. It was shown that a transverse plasma mode occurs in situations where two or more plasma oscillators are put in series. The transverse optical plasmon can be regarded as an out-of-phase oscillation of the two individual components. For $Na_{0.5}CoO_2$, as revealed by neutron experiments [28,29], the magnetic correlations of $Co^{3.5+\delta}$ and $Co^{3.5-\delta}$ are very different, leading to different coupling strengths between two sublattices. When the applied in-plane electric field is perpendicular to the stripes, the situation is similar to the bilayer cuprates with $\boldsymbol{E}\|c$-axis. Effectively, this is like the case of putting the complex

impedances of two sublattices in series, which gives rise to a new transverse mode. Quantitatively, one can use the following formula [32]:

$$\frac{\varepsilon_{av}}{\varepsilon(\omega)} = \frac{\widetilde{Z}_I\omega^2}{\omega(\omega+i\gamma_I)-\omega_I^2} + \frac{\widetilde{Z}_K\omega^2}{\omega(\omega+i\gamma_K)-\omega_K^2} \quad (1)$$

together with $\sigma_1(\omega) = (\omega/4\pi)\mathrm{Im}\,\varepsilon(\omega)$, to fit the conductivity curve. Here, $\widetilde{Z}_I$, γ_I, ω_I and $\widetilde{Z}_K$, γ_K, ω_K are parameters for two plasma oscillators, ε_{av} is another fitting parameter. Without going into details, we can see from Fig. 3 that the model can well reproduce the experimental data. On this basis, the weaker feature appearing at T higher than magnetic ordering or charge ordering transition temperature could be understood as due to the presence of fluctuated charge stripes.

4. *c*-Axis optical response for crystal at the A-type antiferromagnetic region

For $x \geqslant 0.75$, the Na_xCoO_2 enters into another long range magnetic ordering phase at low T (~20 K). The magnetic moment are ferromagnetic correlated within the plane, but antiferromagnetic correlated between the layers, the so-called A-type *AF* ordering. Fig. 4 shows the *c*-axis reflectance spectra for $x = 0.85$ at different temperatures. The reflectance at low frequency increases as the sample is cooled down, evidencing the metallic response. However, when the compound enters into the magnetic ordering phase (below ~20 K), the optical reflectance displays a suppression feature below 230 cm^{-1}. We noticed that the suppression in the *c*-axis $R(\omega)$ is the same as in the *ab*-plane (inset of Fig. 2(b)) both in energy and temperature. It evidences the 3D nature of transport. Based on the results, we can conclude that the *c*-axis dc resistivity must also have an upturn below 20 K. Note that this energy scale is the same as the $x = 0.5$ compound when it enters into the charge ordering phase.

Fig. 5 shows the *c*-axis optical conductivity spectra for $x = 0.85$ sample. Although there is no apparent Drude-like response, the low-frequency conductivity shows finite values, which increases with decreasing temperature, except for the case below 20 K at very low energy. Strong phonon structures appears near 310 and 600 cm^{-1}. They correspond to the two *c*-axis A_{2u} modes. As there are two peaks at each frequency, they are likely originated from

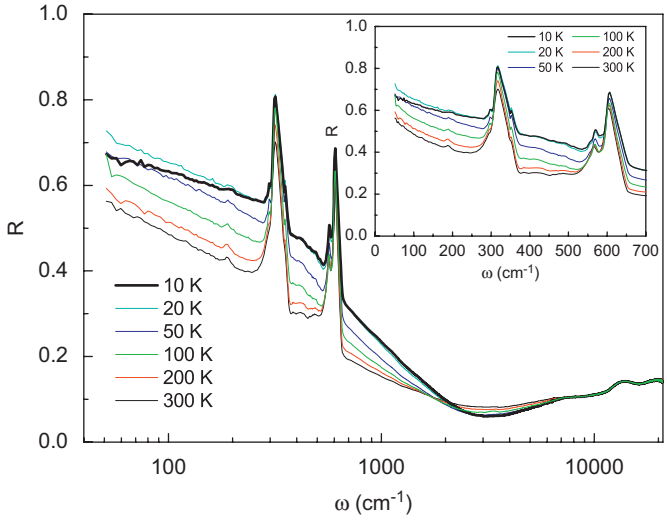

Fig. 4. The *c*-axis reflectance of $x = 0.85$ crystal at different temperatures. The inset is the expanded plot of the reflectance in the far-infrared region. Note that the reflectance is suppressed below 230 cm^{-1} for $T < 20$ K. The suppression appears at the same energy as the in-plane reflectance.

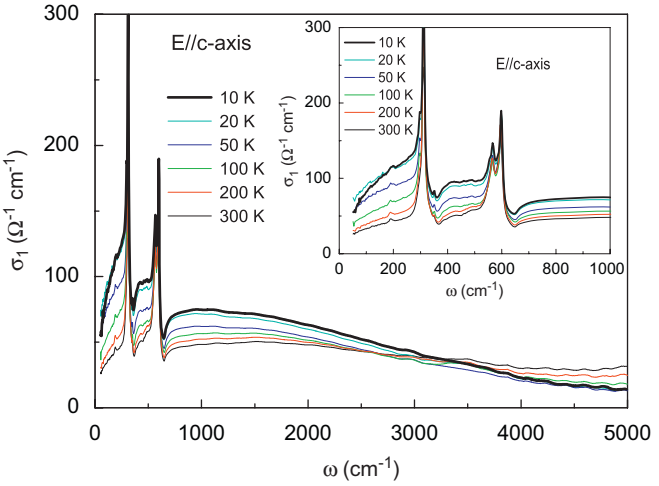

Fig. 5. The *c*-axis conductivity spectra of $x = 0.85$ crystal at different temperatures. The inset is the expanded plot of the conductivity in the far-infrared region.

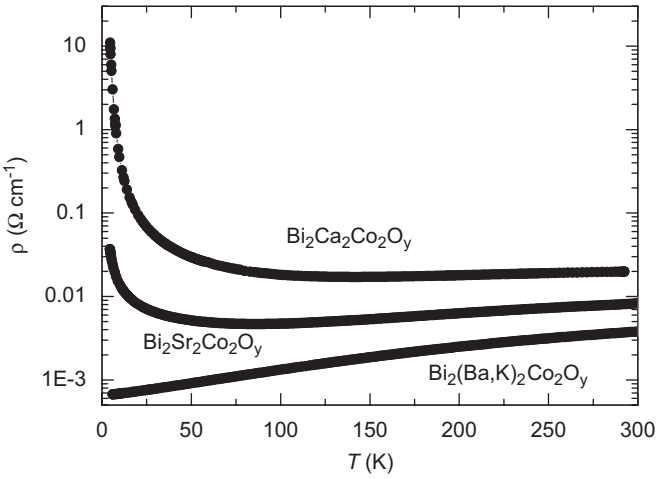

Fig. 6. The temperature-dependent in-plane resistivity for Bi–M–Co–O samples with M = Ba, Sr, Ca.

the occupations of two different Na positions in the crystal structure. The spectra are higher in the low-frequency side than in the high-frequency side for the phonon mode, this is due to the strong coupling between conducting carriers and the lattice. In fact, the broad peak-like structure of conductivity after removing phonon peaks indicates a polaron-like optical response, which also evidences the strong electron–phonon coupling in the system.

5. Optical response of misfit-layered cobaltates

The misfit-layered Bi–M–Co–O and $Ca_3Co_4O_9$ show metallic behavior over a wide temperature range. As M in Bi–M–Co–O changes from Ca to Sr and Ba, the system becomes more metallic. However, all samples, except M = Ba, display an upturn in dc resistivity at low temperature, as shown in Fig. 6. For M = Ba compound, certain amount of *K* element was doped into the sample so that more carriers were introduced. The misfit-layered Bi–M–Co–O compounds are usually identified as $Bi_2M_2Co_2O_y$ (M = Ba, Sr, Ca). The exact chemical compositions of the samples used in our experiment are $[Bi_{1.4}Ca_2Co_{0.6}O_4]^{RS}[CoO_2]_{1.69}$, $[Bi_{1.91}Sr_2O_y]^{RS}[CoO_2]_{1.84}$ and $[Bi_2Ba_{1.3}K_{0.6}Co_{0.1}O_y]^{RS}[CoO_2]_{1.97}$.

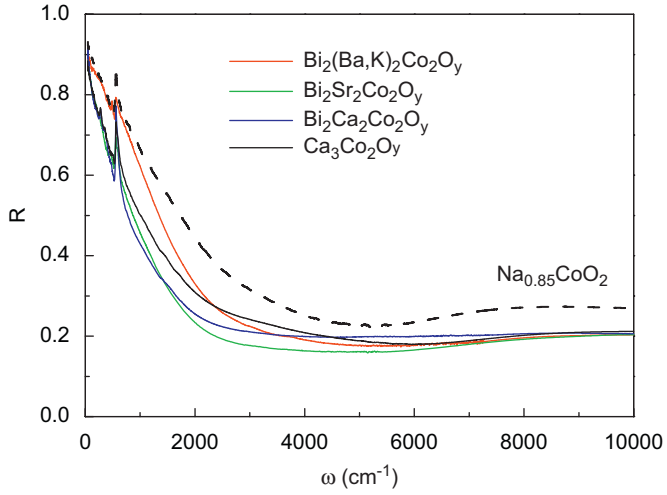

Fig. 7. The in-plane reflectance of Bi–M–Co–O (M = Ba, Sr, Ca) and $Ca_3Co_4O_9$ at room temperature.

A description about crystal growth and characterization can be found in Ref. [34].

Fig. 7 shows the in-plane reflectance for Bi–M–Co–Oand $Ca_3Co_4O_9$ at room-temperature. Even for the most conductive M = Ba system, the optical spectra are similar to those of Na_xCoO_2 with very high Na content ($x>0.9$), indicating their proximity to the band-insulator side. For comparison, the reflectance data for Na_xCoO_2 crystal with $x=0.85$ were also plotted. The temperature-dependent $R(\omega)$ spectra of Bi–M–Co–O are shown in Fig. 8. Basically, all the three samples show metallic behavior, indicated by the high reflectance at low frequency and a dramatic plasma edge in the mid-infrared region. An increase of reflectance is observed as the samples are cooled down through the whole temperature range for Bi–Ba–Co–O and to a certain temperature for Bi–Sr–Co–O and Bi–Ca–Co–O. For the latter two samples, the reflectance gets a depression at low frequency ($<230\,cm^{-1}$) below 100 K which corresponds to the upturn in the T-dependent resistivity curve at low temperature. This phenomenon is also observed in $Ca_3Co_4O_9$ (not shown) and Na_xCoO_2 for high Na contents ($x\geqslant0.75$) shown above, suggesting that the low-T dc resistivity upturn is linked with the weak magnetic ordering [35].

6. Summary

Na_xCoO_2 is a system showing diverse and interesting physical phenomena in different regions of its phase diagram. The evolution of optical spectra with Na doping indicates that the system should be considered as a doped band insulator. However, the electron correlation still plays important role in the system. Spectral features specific to different phases in the phase diagram are presented. For $x\sim0.5$ charge-ordering sample, a small energy gap forms below T_{MIT}. In addition, an electronic resonance develops near $800\,cm^{-1}$ below 100 K. We suggest that this feature corresponds to a new transverse plasma mode. For $x=0.18$ and those with $x\leqslant0.5$ compounds, a pseudogap structure similar to underdoped high-T_c cuprates develops at low temperature. A similar suppression in conductivity also exists in $x>0.5$ compounds, for example $x=0.85$, and misfit-layered cobaltate, but appears at higher energies. When those compounds enter into the A-type antiferromagnetic phase with dc resistivity showing upturns at low temperature, the reflectance is suppressed at the energy similar to $x\sim0.5$ sample in the charge-ordering state.

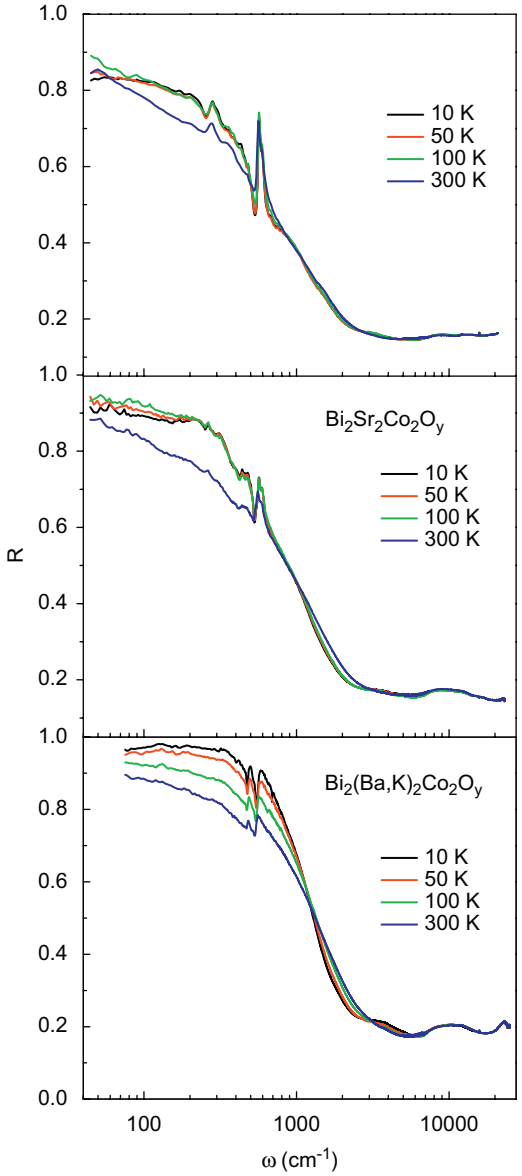

Fig. 8. The temperature-dependent in-plane reflectance of Bi–M–Co–O. The low-frequency reflectance of Bi–Ba–Co–O increases monotonously with decreasing T, indicating a metallic behavior (the bottom panel), while Bi–Sr–Co–O and Bi–Ca–Co–O get suppressed at low frequency below 100 K, corresponds to upturn of low-T dc resistivity (the upper two panels).

Acknowledgments

We thank D. Qian and M.Z. Hasan for their collaboration and discussions on this work. This work is supported by NSFC, the Knowledge Innovation Project of CAS, and the 973 projects of the Ministry of Science and Technology of China. Research at ORNL was sponsored by Material Science and Engineering Division, Office of Basic Energy Sciences, US DOE under contract number DE-AC05-000R22725, managed by UT-Battelle, LLC.

References

[1] M.L. Foo, et al., Phys. Rev. Lett. 92 (2004) 247001.
[2] K. Takada, et al., Nature (London) 422 (2003) 53.
[3] D.J. Singh, Phys. Rev. B 61 (2000) 13397.
[4] R. Jin, et al., Phys. Rev. B 72 (2000) 060512R.
[5] Y. Watanabe, et al., Phys. Rev. B 43 (1991) 3026.
[6] I. Terasaki, et al., Phys. Rev. B 47 (1993) 451.

[7] T. Yamamoto, et al., Jpn. J. Appl. Phys. 39 (2000) L747.
[8] M. Hervieu, et al., Phys. Rev. B 67 (2003) 045112.
[9] A. Maignan, et al., J. Phys. Condens. Matter 15 (2003) 2711.
[10] P. Limelette, et al., Phys. Rev. B 71 (2005) 233108.
[11] S. Lupi, et al., Phys. Rev. B 69 (2004) 180506R.
[12] N.L. Wang, et al., Phys. Rev. Lett. 93 (2004) 237007.
[13] C. Bernhard, et al., Phys. Rev. Lett. 93 (2004) 167003.
[14] G. Caimi, et al., Eur. Phys. J. B 40 (2004) 231.
[15] J. Hwang, et al., Phys. Rev. B 72 (2005) 024549.
[16] N.L. Wang, et al., Phys. Rev. Lett. 93 (2004) 147403.
[17] D. Wu, J.L. Luo, N.L. Wang, Phys. Rev. B 73 (2006) 014523.
[18] C. de Vaulx, M.-H. Julien, C. Berthier, S. Hebert, V. Pralong, A. Maignan, Phys. Rev. Lett. 98 (2007) 246402.
[19] C.A. Marianetti, G. Kotliar, Phys. Rev. Lett. 98 (2007) 246402.
[20] G. Khaliullin, J. Chaloupka, arXiv:0707.2364; J. Chaloupka, G. Khaliullin, arXiv:0708.0543.
[21] P.H. Zhang, et al., Phys. Rev. Lett. 93 (2004) 236402.
[22] K.-W. Lee, et al., Phys. Rev. B 70 (2004) 045104.
[23] M.Z. Hasan, et al., Phys. Rev. Lett. 92 (2004) 246402.
[24] H.B. Yang, et al., Phys. Rev. Lett. 92 (2004) 236403.
[25] D. Qian, et al., Phys. Rev. Lett. 96 (2006) 216405.
[26] D. Qian, et al., Phys. Rev. Lett. 97 (2006) 186405.
[27] M.D. Johannes, I.I. Mazin, D.J. Singh, Phys. Rev. B 71 (2005) 205103.
[28] M. Yokoi, et al., J. Phys. Soc. Jpn. 74 (2005) 3046.
[29] G. Gasparovic, et al., Phys. Rev. Lett. 96 (2006) 046403.
[30] D. van der Marel, A.A. Tsvetkov, Phys. Rev. B 64 (2001) 024530.
[31] M. Gruninger, et al., Phys. Rev. Lett. 83 (2000) 1575.
[32] D. Dulic, et al., Phys. Rev. Lett. 86 (2001) 4144.
[33] D. Munzar, et al., Solid State Commun. 112 (1999) 365.
[34] X.G. Luo, et al., arXiv:0707.2503.
[35] I. Tsukada, T. Yamamoto, M. Takagi, T. Tsubone, S. Konno, K. Uchinokura, J. Phys. Soc. Jpn. 70 (2001) 834.